THE EUROPEAN
PHYSICAL JOURNAL PLUS

Regular Article

Performance comparison of capacitance-based flowmeter with gamma-ray attenuation-based two-phase flowmeter for determining volume fractions in an annular flow regime's components

Mohammadmehdi Roshani[1,2], **Giang T. T. Phan**[1], **Ehsan Nazemi**[3],
Ehsan Eftekhari-Zadeh[4], **Nhut-Huan Phan**[1], **Enrico Corniani**[5,6,a] [ID],
Hoai-Nam Tran[1], **Van Hao Duong**[7], **Gholam Hossein Roshani**[8]

[1] Institute of Fundamental and Applied Sciences, Duy Tan University, Ho Chi Minh City 700000, Vietnam
[2] Faculty of Electrical – Electronic Engineering, Duy Tan University, Da Nang 550000, Vietnam
[3] Imec-Vision Lab, Department of Physics, University of Antwerp, Antwerp, Belgium
[4] Institute of Optics and Quantum Electronics, Friedrich-Schiller-University Jena, Max-Wien-Platz 1, Jena 07743, Germany
[5] Division of Nuclear Physics, Advanced Institute of Materials Science, Ton Duc Thang University, Ho Chi Minh City, Vietnam
[6] Faculty of Applied Sciences, Ton Duc Thang University, Ho Chi Minh City, Vietnam
[7] Hanoi University of Mining and Geology, No 18, Vien street, Bac Tu Liem District, Hanoi, Vietnam
[8] Electrical Engineering Department, Kermanshah University of Technology, Kermanshah, Iran

Abstract Precise metering of the void fraction is one of the important problems in the oil, chemical and petrochemical industries. For void fraction measurement, there are different kinds of sensors with different configurations. In this regard, the capacitance-based sensor and gamma-ray attenuation-based sensor are very well known as two most accurate and widely used sensors. In this paper, we report, to the best of our knowledge, for the first time a comparison between these two sensors in an annular air–oil flow. Simulations were accomplished with benchmarked COMSOL Multiphysics software and MCNPX code. Results show that the general sensitivity of gamma-ray sensor is ~ 90% higher than the general sensitivity of capacitance-based sensor. For a more accurate comparison, momentary sensitivity factors for a variety void fractions in both sensors were obtained. In the low void fraction range, the gamma-ray sensor has much better performance; however, in the high void fraction range, the capacitance-based sensor has a better performance. In the range of 0.9–1 void fractions, the momentary sensitivity of capacitance-based sensor is ~ 67% higher than that of gamma-ray attenuation-based sensor.

1 Introduction

Exact determination of phase percentage in two-phase flows remains as one of the challenging problems in the oil, chemical and petrochemical industries. In this regard, there are

---

[a] e-mail: enrico.corniani@tdtu.edu.vn (corresponding author)

 Springer

different kinds of sensors with various efficiencies. The application of capacitance-based sensor for determining the phase percentage in multi-phase flows was introduced by Sami and his coworkers in 1980 [1]. They investigated a number of capacitance designs in two-phase pipelines and then compared the experimental results. It was concluded that in a specified flow regime, a four-concave-plate structure is preferential for having a higher sensitivity and later on for simplicity in the construction. In the same year, determination of the phase percentages in multi-phase systems using gamma-ray attenuation was presented by Abouelwafa and his coworker [2]. It was concluded that the described method is a simple and accurate way of determining the volume fractions of multi-phase flows. The design methodology of capacitance-based sensors for void fraction measurement was investigated by Ahmed in adiabatic two-phase flow schemes [3]. A theoretical and experimental investigation was conducted on two different sensor configurations, i.e., concave and ring types, to study the influence of design factors on the capacitance output. A linear correlation between output capacitance and void fraction was understood for both types of sensors.

A capacitive sensing system was introduced in 2017 in order to measure the void fraction in gas–oil two-phase flow configuration [4]. Double-ring and concave electrodes were employed and compared to each other. Dependency of outputs of the electrodes on flow regime, especially in concave configuration, was verified by experimental results. Salehi and his coworkers investigated different electrode configurations for oil–air two-phase flow measurement for different flow regimes [5]. The results showed a different sensitivity for each electrode shape. In annular configuration, concave shape was found to be more sensitive than the other ones. Salehi et al. proposed a twin rectangular fork-like capacitance (TRFLC) sensor in order to recognize the flow pattern of gas–oil two-phase flow in a horizontal pipe [6]. The required simulations in [6] were performed using COMSOL software.

There are a lot of studies in the field of applications of gamma-ray attenuation-based techniques for determining the phase fractions. Salgado and his coworkers presented several radiation-based metering systems for a number of objectives in multi-phase flows using artificial neural network [7–9]. They used mainly MCNP and MATLAB software applications. Mosorov and his coworkers presented a gamma-ray-based measuring system and modeled a dynamic flow using MCNP5 code [10]. Hanus et al. studied several metering systems by focusing on soft computing. They used different transforms such as Hilbert and Fourier, different feature extraction methods and also different kinds of ANNs [11–13]. In 2019, a simple and affordable design for volume fraction prediction in stratified three-phase flowmeter using single source and single detector was introduced [14, 15]. Roshani and his coworkers presented a large number of ANNs in order to specify phase fractions in multi-phase flows. All of the simulations were typically performed using MCNPX code and MATLAB software [16–28]. From 1980 up to now, many researchers have conducted many studies in this field; however, to the best knowledge of the authors, there is no direct comparison between capacitance-based sensor and gamma-ray attenuation-based sensor. This paper will start presenting a benchmarking of COMSOL simulation and MCNP code. In the following part, a concave capacitance-based sensor and gamma-ray attenuation-based sensor using Cs-137 and NaI detector are simulated in a common situation and the general and momentary sensitivities are then compared to each other.

2 Benchmark of simulations

In this study, two different software applications, i.e., COMSOL and MCNP, were used in order to simulate the capacitance-based sensor and gamma-ray attenuation-based sensor in
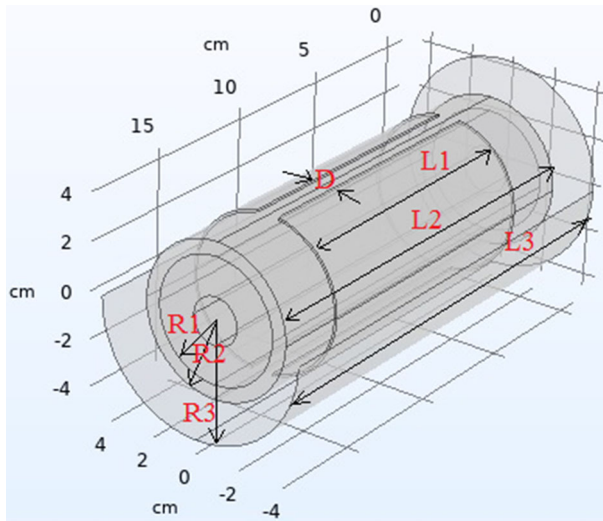
Fig. 1 The schematic of the structure used for validation of the COMSOL simulation

air–oil two-phase flow, respectively. For this purpose, the simulations were initially bench-marked according to references [5, 20].
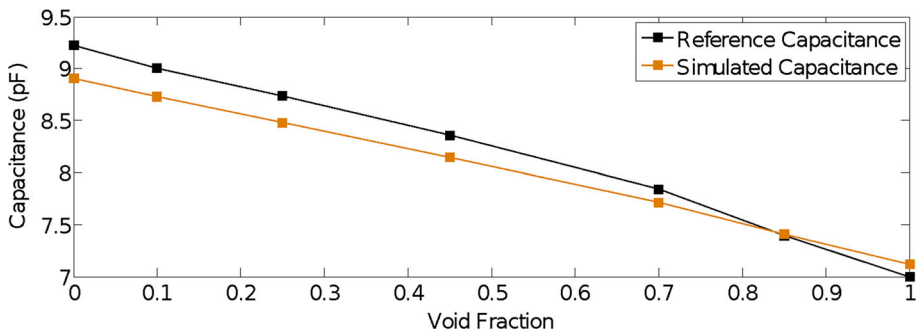
2.1 COMSOL benchmark

In order to benchmark the COMSOL simulation, an experimental study and a numerical study were used [5]. In this study, an experimental investigation and a numerical study have been performed on different electrode configurations for air–oil two-phase flow measurement in various patterns. In the present study, a concave capacitance-based sensor with the specified configuration in [5] was initially simulated and then the results of COMSOL simulation for concave electrode were compared with those achieved by MCNP. The electrodes (one for exciting and one as measuring) made from soft copper with a 0.1 cm thickness were considered. The inner radius of the test pipe is R1 = 2.6 cm, the outer radius of the pipe is R2 = 3.2 cm, the radius of considered earth is R3 = 4.5 cm, the length of electrodes is L1 = 12 cm, the length of pipe is L2 = 18 cm, the length considered for earth is L3 = 20 cm and the distance between electrodes is D = 1 cm. Meanwhile, the relative permittivities of air, oil and pipe wall are set as 1, 2.2 and 3.3, respectively. The simulated structure for validation of the COMSOL simulation is depicted in Fig. 1.

The annular air–oil two-phase flow was considered, and the simulations were carried out in the void fractions of 0, 0.1, 0.25, 0.45, 0.70, 0.85 and 1. The comparison of COMSOL simulation with the results presented in reference [5] is given in Table 1 and is graphed in Fig. 2 and clearly shows a good agreement between the COMSOL simulation and the experimental data.

The average relative difference of simulated capacitance and reference capacitance was ~0.022 which is a relatively low value. This negligible discrepancy could be attributed to the considered earth or the length of the test pipe which has not been mentioned clearly in reference [5]. These results indicate the validation of the simulated results.

Table 1 The comparison of the results calculated by COMSOL simulation with [5] for validation of the simulation

Void fraction	Reference capacitance [5] (pF)	Simulated capacitance with COMSOL (pF)	Relative difference
0	9.22	8.9	0.034
0.1	9	8.73	0.030
0.25	8.74	8.48	0.029
0.45	8.36	8.14	0.026
0.7	7.84	7.71	0.016
0.85	7.39	7.41	0.002
1	7	7.12	0.017

Fig. 2 The comparison of the results calculated by COMSOL simulation with [5] for validation of the simulation

2.2 MCNP benchmark

In order to validate the MCNP simulation, several experiments which had been already carried out in reference [29] for the case of annular flow regime were used as benchmark. The mentioned experimental setup was simulated using MCNP for benchmarking the simulation. The setup consists of a Pyrex glass pipe with an inner radius of 4.75 cm (R1 = 4.75 cm), length of 40 cm (L1 = 40 cm) and wall thickness of 0.25 cm (D1 = 0.25 cm) as the main pipe. A 2 mCi (74 MBq) Cs-137 radioisotope source was located 30 cm far from the pipe (L2 = 30 cm) together with one NaI detector with the dimensions of 1×1 inch which was placed 20 cm away from the pipe (L3 = 20 cm). This configuration was simulated to ensure the same conditions of experimental setup in reference [29] and also in our simulation. Furthermore, a cubic collimator with 0.6 cm in width, 2 cm in height and 10 cm in length was considered. The simulated setup is shown in Fig. 3. Gasoil (chemical formula of $C_{12}H_{23}$ and density of 0.826 g/cm^3) and air were considered as the liquid and gas phases, respectively, similarly as in the aforementioned experiment. Void fractions of 0, 0.2, 0.3, 0.4, 0.5, 0.6 and 0.7 were simulated, and then the results were compared.

Registered counts in detector were calculated per one source particle in the MCNPX code using Pulse Height Tally F8. Registered counts in MCNP are per source particle, and for this reason the simulated and experimental data were normalized to one. For terminating calculations in a specified tally precision, the "STOP" card was used. A maximum 0.01
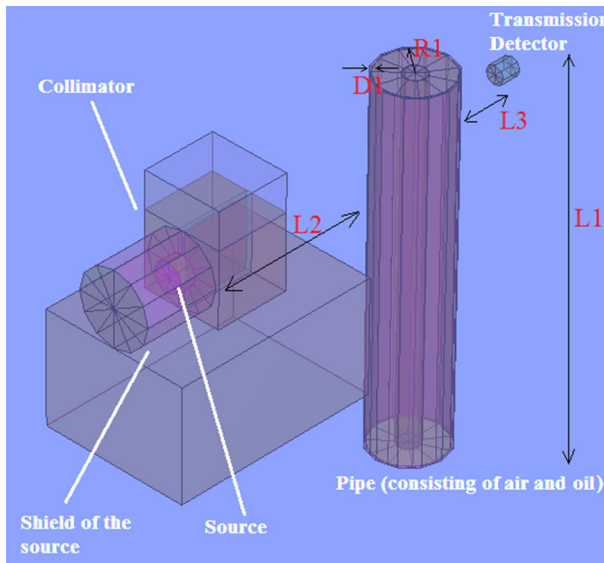
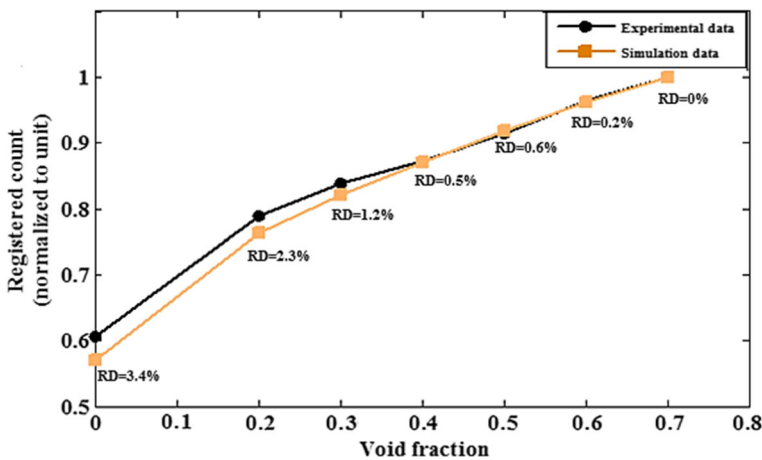**Fig. 3** The simulated setup similar to the conditions mentioned in the performed experimental setup

Fig. 4 Comparison of the experimental data and the simulated data in two-phase annular flow

relative error in all of the simulations was set using this card; consequently, all of the Monte Carlo results meet this standard of precision. Comparison of experimental data and simulation data in two-phase annular flow is shown in Fig. 4. As can be implied from the figure, the MCNP simulation is in a good agreement with the results presented in reference [29] which shows the validation of our simulated results. The maximum relative difference between experimental and simulated results was 3.4%, and the mean relative difference of simulations and experiments was 0.011 which is a very low difference. This negligible difference could be attributed to the inevitable constructional details in the annular regime of phantoms which can only be observed in the experiments. In fact, the dimensions of phantoms are not exactly the same as the simulated geometry.

3 Simulation

Using the COMSOL simulation, an air content was defined in the simulated model since significant fringing fields may be observed around the capacitor plates. In other words, the fringing electric fields may increase to infinity, although they decrease cubically in proportion to the inverse of the distance. They can quickly become infinity small enough to be numerically assumed negligible. A 3D model in the electrostatic physics (AC/DC > Electric Fields and Currents > Electrostatics (es)) was made up. The stationary regime was used for the simulation. In this regime, variables related to the field are constant over the course of time.

In the MCNP simulation, Pulse Height Tally F8 is normally used to calculate the recorded counts per source particle in the NaI detector. To save time in running the code, the STOP card was deployed in the code in order to terminate the calculation process as soon as a desired tally precision was acquired. A maximum relative error of 0.01 was set in all simulations using the same STOP card to ensure that all Monte Carlo results satisfy this precision standard.

For comparison of the performance of the capacitance-based sensor and gamma-ray attenuation-based sensor, a typical structure was simulated using the benchmarked COMSOL and MCNP software. A Pyrex glass pipe with an inner radius of 4.75 cm, length of 40 cm, wall thickness of 0.25 cm and relative permittivity of 4.7 was considered as the main pipe. A capacitance-based sensor with the electrodes made of soft copper and 0.1 cm thickness and 12 cm length was modeled. The distance between electrodes was considered 1 cm. A gamma-ray attenuation-based sensor with 2 mCi Cs-137 source located 30 cm far from the pipe and one 1×1 inch NaI detector located 20 cm far from the pipe were programmed into the simulation. Gasoil (chemical formula of $C_{12}H_{23}$ and density of 0.826 g/cm^3 and relative permittivities of 2.1) and air were considered as the liquid and gas phases, respectively. The simulated structure, the meshed model and the electric potential distribution of capacitance-based sensor in a typical void fraction are illustrated in Fig. 5.

The simulated structure in MCNP code for obtaining the sensitivity of gamma-ray attenuation-based sensor and the registered interactions with the material (particle track) in a typical void fraction is illustrated in Fig. 6.

The computer used to run the COMSOL and MCNP simulations was an Intel Core i7-3537U CPU @ 2.50 GHz and 6.00 GB of RAM. Computational time for MCNP simulation in void fraction of 0.5 was 2:03':50", and computational time for COMSOL simulation in this void fraction was 0:0':11". The MCNP is a Monte Carlo-based code, and the COMSOL Multiphysics is a cross-platform finite element analysis software; for this reason, the calculation time of these tools is so different.

In order to make a fair comparison between these two different sensors, general sensitivity factor for the whole range of void fractions (0–1) and momentary sensitivity factor for the void fraction ranges of 0–0.1, 0.1–0.2, 0.3–0.4, 0.4–0.5, 0.5–0.6, 0.6–0.7, 0.7–0.8, 0.8–0.9 and 0.9–1 were defined as follows:

$$\text{General Sensitivity Fact} = \frac{\text{maximum output of the sensor} - \text{minimum output of the sensor}}{\text{maximum output of the sensor}} \tag{1}$$
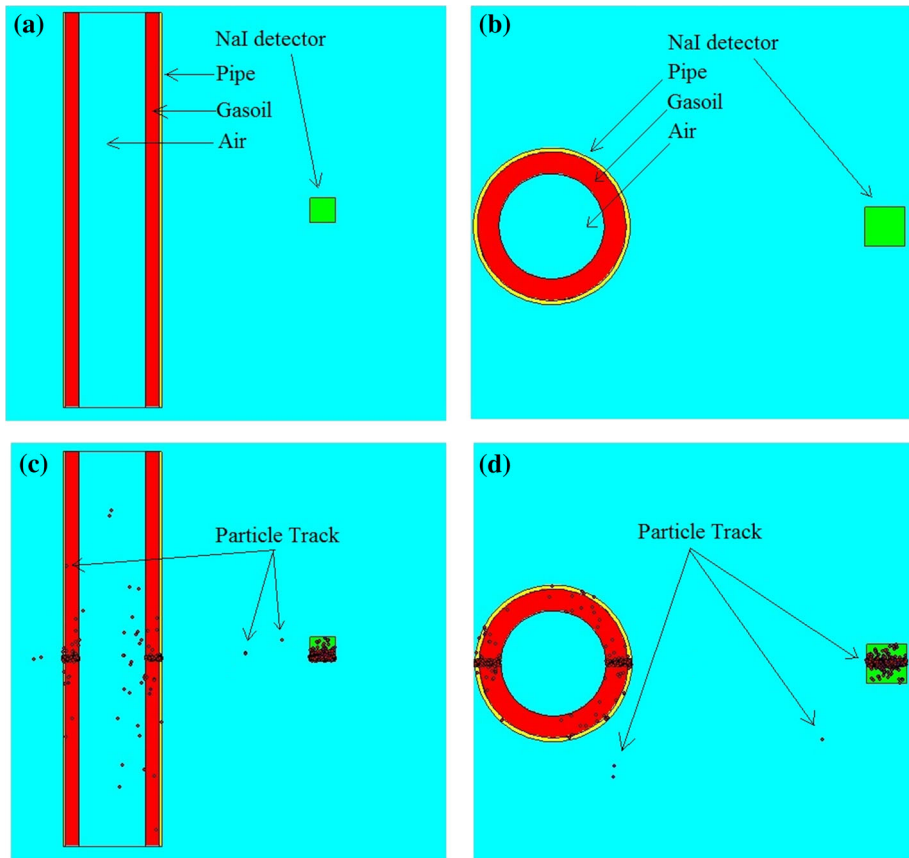
$$\text{Momentary Sensitivity Factor} = \frac{\text{maximum output of the sensor in specified range} - \text{minimum output of the sensor in specified range}}{\text{maximum output of the sensor in specified range}}. \tag{2}$$
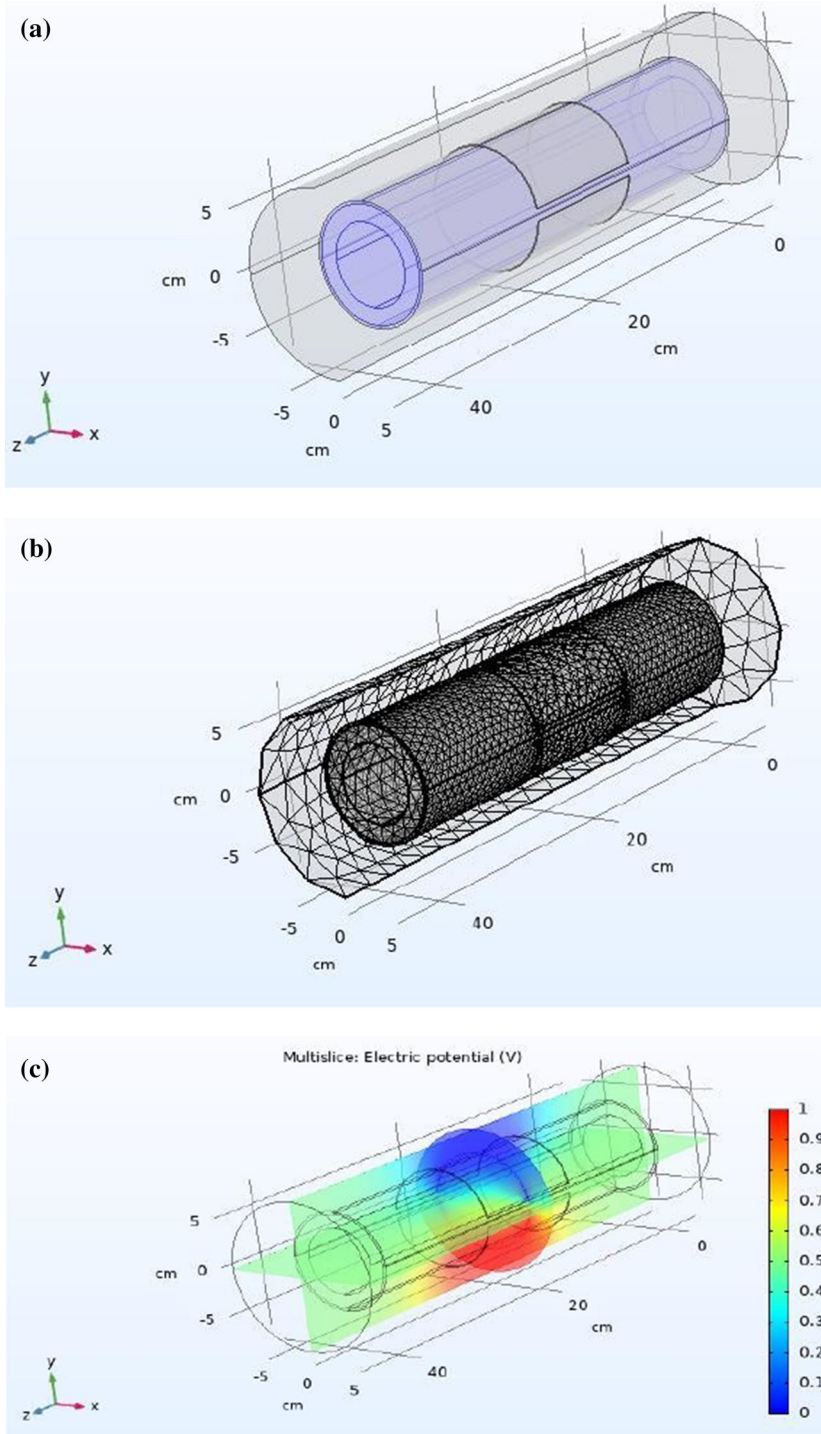
Fig. 5 a Simulated structure of capacitance-based sensor, **b** meshed model of capacitance-based sensor and **c** electric potential distribution of capacitance-based sensor

Fig. 6 a Simulated structure in MCNP code (XZ), **b** simulated structure in MCNP code (XY), **c** particle track (XZ), **d** particle track (XY)

The void fractions from 0 to 1 in steps of 0.1 were simulated for both sensors, and the results will be presented in the next section.

4 Results and discussion

The results of capacitance and gamma-ray attenuation-based sensors for the different void fractions are shown in Fig. 7 and are given in Table 2.

As can be seen in Fig. 7 and Table 2, the general sensitivity factor of capacitance-based sensor is 0.261 and the general sensitivity of gamma-ray attenuation-based sensor is 0.495. General sensitivity of gamma-ray sensor is 90% higher than that of capacitance-based sensor, which proves the strong ability of gamma-ray attenuation-based sensor in void fraction metering of annular air–oil flows.

According to Fig. 7, the average slope of gamma-ray attenuation-based sensor output is larger on the whole range, but in some specified ranges the slope of capacitance-based sensor output is higher. Therefore, momentary sensitivities of capacitance and gamma-ray
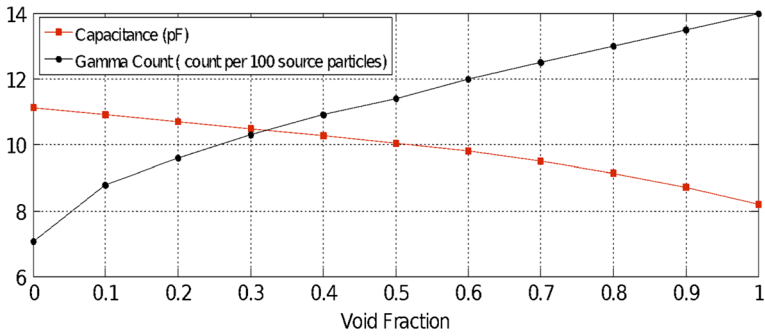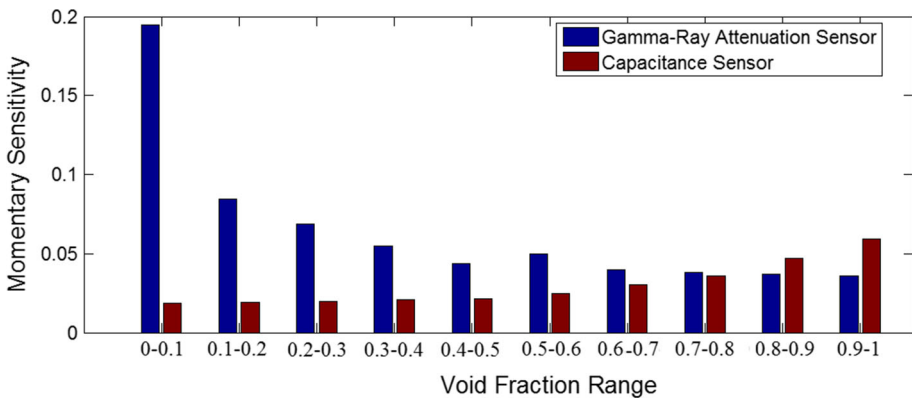
Fig. 7 Results of capacitance and gamma-ray attenuation-based sensors for different void fractions

Table 2 Results of capacitance and gamma-ray attenuation-based sensors for the void fraction in the range 0–1

Void fraction	Capacitance (pF)	Gamma count (count per 100 source particles)
1	8.2	14
0.9	8.72	13.5
0.8	9.15	13
0.7	9.49	12.5
0.6	9.79	12
0.5	10.04	11.4
0.4	10.26	10.9
0.3	10.48	10.3
0.2	10.69	9.59
0.1	10.9	8.78
0	11.11	7.07

Fig. 8 Momentary sensitivity of capacitance-based and gamma-ray attenuation-based sensors for the different ranges of void fractions

attenuation-based sensors in different ranges of void fractions were compared to each other. These results are given in Table 3 and are shown in Fig. 8.

Table 3 Momentary sensitivity of capacitance and gamma-ray attenuation-based sensors for the different ranges of void fractions

Void fraction range	Momentary sensitivity of capacitance-based sensor	Momentary sensitivity of gamma-ray attenuation-based sensor
0–0.1	0.0189	0.1947
0.1–0.2	0.0192	0.0844
0.2–0.3	0.0196	0.0689
0.3–0.4	0.0209	0.055
0.4–0.5	0.0214	0.0438
0.5–0.6	0.0249	0.05
0.6–0.7	0.0306	0.04
0.7–0.8	0.0358	0.0384
0.8–0.9	0.0469	0.037
0.9–1	0.0596	0.0357

As shown in Fig. 8 and Table 3, in some cases the momentary sensitivity factor of the capacitance-based sensor is higher than that of the gamma-ray attenuation-based sensor. For example, in the void fraction range of 0.9–1, the momentary sensitivity of capacitance-based sensor is 67% higher than that of gamma-ray attenuation-based sensor, which shows the better performance of capacitance-based sensor in high ranges of void fraction. It should be noted that this behavior was obtained for annular regime of air–oil flow, and for other regimes like in stratified or homogeneous the behavior might be different.

5 Conclusion

In this paper, two different well-known sensors in multi-phase flow metering industry were compared. The performance of gamma-ray attenuation-based sensor and capacitance-based sensor in the annular air–oil two-phase flow was investigated. For this purpose, a finite element (FE) simulation software (COMSOL Multiphysics) and a Monte Carlo code (MCNPX) were employed. Firstly, the simulations were benchmarked by comparing them with the approved studies. The mean relative differences of simulated structure by COMSOL and MCNP codes with previous approved studies were 0.022 and 0.011, respectively, which proves the validation of simulations. The general sensitivity factor of concave capacitance and gamma-ray attenuation-based sensors was obtained 0.261 and 0.495, respectively. General sensitivity of gamma-ray sensor is 90% higher than that of concave capacitance-based sensor, which shows the strong ability of gamma-ray attenuation-based sensor in void fraction metering of annular air–oil two-phase flows. Moreover, the momentary sensitivity of the sensors was obtained in different void fractions and the results showed that the concave capacitance-based sensor has a better performance in 0.8–1 void fraction.

References

1. M.S.A. Abouelwafa, E.J.M. Kendall, The use of capacitance sensors for phase percentage determination in multiphase pipelines. IEEE Trans. Instrum. Meas. **29**(1), 24–27 (1980)

2. M.S.A. Abouelwafa, E.J.M. Kendall, The measurement of component ratios in multiphase systems using alpha-ray attenuation. J. Phys. E Sci. Instrum. **13**(3), 341 (1980)

3. H. Ahmed, Capacitance sensors for void-fraction measurements and flow-pattern identification in air–oil two-phase flow. IEEE Sens. J. **6**(5), 1153–1163 (2006)

4. S.M. Salehi, H. Karimi, A.A. Dastranj, A capacitance sensor for gas/oil two-phase flow measurement: exciting frequency analysis and static experiment. IEEE Sens. J. **17**(3), 679–686 (2016)

5. S.M. Salehi, H. Karimi, R. Moosavi, A.A. Dastranj, Different configurations of capacitance sensor for gas/oil two phase flow measurement: an experimental and numerical study. Exp. Therm. Fluid Sci. **82**, 349–358 (2017)

6. S.M. Salehi, H. Karimi, A.A. Dastranj, R. Moosavi, Twin rectangular fork-like capacitance sensor to flow regime identification in horizontal co-current gas-liquid two-phase flow. IEEE Sens. J. **17**(15), 4834–4842 (2017)

7. C.M. Salgado, C.M. Pereira, R. Schirru, L.E. Brandão, Flow regime identification and volume fraction prediction in multiphase flows by means of gamma-ray attenuation and artificial neural networks. Prog. Nucl. Energy **52**(6), 555–562 (2010)

8. C.M. Salgado, L.E. Brandão, C.M. Pereira, W.L. Salgado, Salinity independent volume fraction prediction in annular and stratified (water–gas–oil) multiphase flows using artificial neural networks. Prog. Nucl. Energy **76**, 17–23 (2014)

9. C.M. Salgado, L.E.B. Brandão, C.C. Conti, W.L. Salgado, Density prediction for petroleum and derivatives by gamma-ray attenuation and artificial neural networks. Appl. Radiat. Isot. **116**, 143–149 (2016)

10. Mosorov, et al., Modelling of dynamic experiments in MCNP5 environment. Appl. Radiat. Isot. **112**, 136–140 (2016)

11. R. Hanus, Application of the Hilbert transform to measurements of liquid–gas flow using gamma ray densitometry. Int. J. Multiph. Flow **72**, 210–217 (2015)

12. R. Hanus, M. Zych, L. Petryka, D. Świsulski, A. Strzępowicz, Application of ANN and PCA to two-phase flow evaluation using radioisotopes, in *EPJ Web of Conferences,* vol. 143 (EDP Sciences, 2017), p. 02033

13. R. Hanus, M. Zych, M. Kusy, M. Jaszczur, L. Petryka, Identification of liquid-gas flow regime in a pipeline using gamma-ray absorption technique and computational intelligence methods. Flow Meas. Instrum. **60**, 17–23 (2018)

14. R.G. Peyvandi, A simple and inexpensive design for volume fraction prediction in three-phase flow meter: single source-single detector. Flow Meas. Instrum. **69**, 101587 (2019)

15. R.G. Peyvandi, S.I. Rad, Application of artificial neural networks for the prediction of volume fraction using spectra of gamma rays backscattered by three-phase flows. Eur. Phys. J. Plus **132**(12), 511 (2017)

16. M. Roshani, G. Phan, G.H. Roshani, R. Hanus, B. Nazemi, E. Corniani, E. Nazemi, Combination of X-ray tube and GMDH neural network as a nondestructive and potential technique for measuring characteristics of gas–oil–water three phase flows. Measurement **168**, 108427 (2021)

17. M. Roshani, G.T. Phan, P.J.M. Ali, G.H. Roshani, R. Hanus, T. Duong, E. Corniani, E. Nazemi, E.M. Kalmoun, Evaluation of flow pattern recognition and void fraction measurement in two phase flow independent of oil pipeline's scale layer thickness. Alexandria Eng. J. **60**, 1955–1966 (2021)

18. M. Roshani, M.A. Sattari, P.J.M. Ali, G.H. Roshani, B. Nazemi, E. Corniani, E. Nazemi, Application of GMDH neural network technique to improve measuring precision of a simplified photon attenuation based two-phase flowmeter. Flow Meas. Instrum. **75**, 101804 (2020)

19. M. Roshani, G. Phan, R.H. Faraj, N.H. Phan, G.H. Roshani, B. Nazemi, E. Corniani, E. Nazemi, Proposing a gamma radiation based intelligent system for simultaneous analyzing and detecting type and amount of petroleum by-products. Nucl. Eng. Technol. (2020). https://doi.org/10.1016/J.NET.2020.09.015

20. A. Karami, G.H. Roshani, A. Khazaei, E. Nazemi, M. Fallahi, Investigation of different sources in order to optimize the nuclear metering system of gas–oil–water annular flows. Neural Comput. Appl. **32**(8), 3619–3631 (2020)

21. G.H. Roshani, S. Roshani, E. Nazemi, S. Roshani, Online measuring density of oil products in annular regime of gas–liquid two phase flows. Measurement **129**, 296–301 (2018)

22. E. Nazemi, S.A.H. Feghhi, G.H. Roshani, R.G. Peyvandi, S. Setayeshi, Precise void fraction measurement in two-phase flows independent of the flow regime using gamma-ray attenuation. Nucl. Eng. Technol. **48**(1), 64–71 (2016)

23. G.H. Roshani, E. Nazemi, M.M. Roshani, Intelligent recognition of gas-oil-water three-phase flow regime and determination of volume fraction using radial basis function. Flow Meas. Instrum. **54**, 39–45 (2017)

24. E. Nazemi, G.H. Roshani, S.A.H. Feghhi, S. Setayeshi, E.E. Zadeh, A. Fatehi, Optimization of a method for identifying the flow regime and measuring void fraction in a broad beam gamma-ray attenuation technique. Int. J. Hydrog. Energy **41**(18), 7438–7444 (2016)

25. G.H. Roshani, E. Nazemi, M.M. Roshani, Flow regime independent volume fraction estimation in three-phase flows using dual-energy broad beam technique and artificial neural network. Neural Comput. Appl. **28**(1), 1265–1274 (2017)
26. G.H. Roshani, E. Nazemi, M.M. Roshani, Identification of flow regime and estimation of volume fraction independent of liquid phase density in gas-liquid two-phase flow. Prog. Nucl. Energy **98**, 29–37 (2017)
27. G.H. Roshani, E. Nazemi, S.A.H. Feghhi, Investigation of using 60Co source and one detector for determining the flow regime and void fraction in gas–liquid two-phase flows. Flow Meas. Instrum. **50**, 73–79 (2016)
28. G.H. Roshani, E. Nazemi, Intelligent densitometry of petroleum products in stratified regime of two phase flows using gamma ray and neural network. Flow Meas. Instrum. **58**, 6–11 (2017)
29. G.H. Roshani, E. Nazemi, S.A.H. Feghhi, S. Setayeshi, Flow regime identification and void fraction prediction in two-phase flows based on gamma ray attenuation. Measurement **62**, 25–32 (2015)